Bulletin of the Seismological Society of America, Vol. 99, No. 2B, pp. 1333–1342, May 2009, doi: 10.1785/0120080123

Interpretation of Broadband Ocean-Bottom Seismometer Horizontal Data Seismic Background Noise

by Robert Pillet, Anne Deschamps, Denis Legrand, Jean Virieux,* Nicole Béthoux, and Ben Yates

Abstract The seismic background noise observed on the OBS (ocean-bottom seismometer) recordings is well known to be strong. With the recent appearance of broadband OBS, the background noise in the extended frequency range is even more significant. By taking into account the various degrees of freedom of the seismic sensors, it has been shown that the seismometers are not only translational sensors but also rotational ones with a sensitivity that depends on the installation. The strong similarity of the background noise recorded on the two horizontal traces of the broadband Hippocampe OBS data deployed during the Rosmarin program is interpreted as a rotational motion around the vertical axis. This torsion motion is so important that it dominates the other noise seismic contributions like translations and tilt (rotational motion around a horizontal axis) and represents more than 90% of the background noise signal at the periods between 5 and 50 sec.

Use of the difference between the two horizontal traces makes it possible to reduce the background noise made up primarily of this torsion motion and thus to enhance the displacement signal but also strongly modify it. An effort should be made to better control the installation of the sensors on the seafloor. A better solution would be to simultaneously record rotations at the same position as that of the seismometer. Such data will permit the correction of the seismic traces of the OBS data and strongly reduce the background noise.

Introduction

The fabrication of an ocean-bottom seismometer (OBS) represents a series of compromises to obtain reliable data at relatively low cost. The first broadband seismic data from the seafloor were obtained in the mid1960s (Sutton *et al.*, 1965) with a large budget but located only in a few places. In order to improve Earth coverage the number and quality of OBS have been significantly increased in the 1990s (Suyehiro *et al.*, 1992; Montagner *et al.*, 1994a,b; Beaudouin *et al.*, 1996a; Bradley *et al.*, 1997; Laske, 1998; Romanowicz *et al.*, 1998). An important point in processing these data is to understand the noise as proposed by Longuet-Higgins (1950) where he explained the micro seismic peak of around a 14 sec period as the coupling of oceanic stationary waves with the surface of the ocean floor. The 1998 Ocean Seismic Network Pilot Experiment offered a unique opportunity to observe the effect of seismometer emplacement on broadband data quality (Stephen *et al.*, 2003). The high coherence between pressure and seismic signals in the seismic period band is well known and has been used for both land broadband seismometers and OBS. Beauduin *et al.* (1996) corrected the effect of atmospheric pressure changes on the broadband seismometers. Crawford *et al.* (1991) developed a technique that uses the coherence between OBS data and local pressure change under the loading of long-period ocean waves to study crustal structure under the station. Stutzmann *et al.* (2001) showed that the diurnal variations of the vertical seismic component can be efficiently removed by subtracting the effect of the horizontal components without any theoretical explanation. As far as the low frequency noise recorded at seafloor and borehole sites comes from instrument tilting under fluid flow, it can be greatly reduced on the vertical component by removing the noise-coherent part on the horizontal component (Crawford and Webb, 2000; Stutzmann *et al.*, 2001; Dahm *et al.*, 2006). Some stations record strong noise at frequencies below 0.1 Hz, which could be attributed to tilt-induced noise. The authors previously quoted offer practical solutions to the reduction of the OBS seismic background noise using a combination of signals of the three components and pressure measurement, but they do not give any theoretical explanations to explain why their techniques are effec-

*Present address: Laboratoire Géophysique Interne et Tectonophysique, Université Joseph Fourier, BP 53, 38041 Grenoble, Cedex 9, France.

tive. We propose here some theoretical explanations for this noise reduction in broadband seismometer data.

Recording Campaign

Data analyzed in this article were obtained during the summer of 2006 OBS deployment of the Rosmarin program, a microseismicity observation program in the Ligurian Sea in front of the French Rivera developed by Geosciences Azur (Observatoire Océanologique de Villefranche sur Mer) from 2001 to 2006. Three OBS have been deployed in periods of two months, two or three times per year above the studied area to simulate a permanent small seismological network. Recently, the OBS have been upgraded, and the Hippocampe OBS (Charvis and Hello, 2005) connected to broadband CMG-40TOBS sensors from Güralp, especially adapted for such marine environments, have been deployed. The summer 2006 data are obtained on three instruments, which provided a continuous record on a 24-bit digitizer at 100 samples per second at sites STA1, STA2, and STA3 in *a priori* similar soil conditions at depths from 1000 to 2000 m. A combination of autolevelling electronics and a gimbal of ±120° range ensures the verticality of the system over any seafloor surface. There is no control on the horizontal components orientation; we keep the notation x, y for these two components, which are not representing north–south and east–west motions but two arbitrary perpendicular horizontal orientations noted as H1 and H2.

Seismometer Description

The Güralp CMG-40TOBS seismometers are built around an inverted pivoting pendulum (Fig. 1), an electronic feedback, hence a flat broadband response up to a 40 sec period (Fig. 2).

The pivoting pendulum used by Güralp Systems Limited is an inertial sensor constructed with a rigid articulated arm at one end carrying the proof mass at the other end. Depending on the arm and pivot axis orientation, such a mechanical system can describe all kinds of seismometers. The horizontal arm and pivot axes give the vertical pendulums, models equivalent to those developed by Galitzine (1912) and LaCoste (1934). The horizontal arm and vertical pivot axis give the horizontal garden-gate model as the STS1-H Streckeisen seismometer. Vertical up, or down, arm and horizontal pivot axis give the simple or inverted pendulum. The inverted pendulum was developed by Wiechert (1903) and taken up again by Güralp Systems Limited. The definition of one of the three 120° components of the STS-2 seismometer from Streckeisen is 35° from the vertical inclined arm and horizontal pivot axis. This symmetric triaxial configuration was first proposed by Galperin (1985).

The equations of a pivoting pendulum have already been written by Galitzine (1912), Byerly (1952), Rodgers (1968), Bradner and Reichle (1973), Trifunac and Todorovska (2001), Graizer (2005, 2006) and Graizer and Kalkan (2008). In the case of an inverted horizontal pivoting pendulum (Fig. 1), these equations are

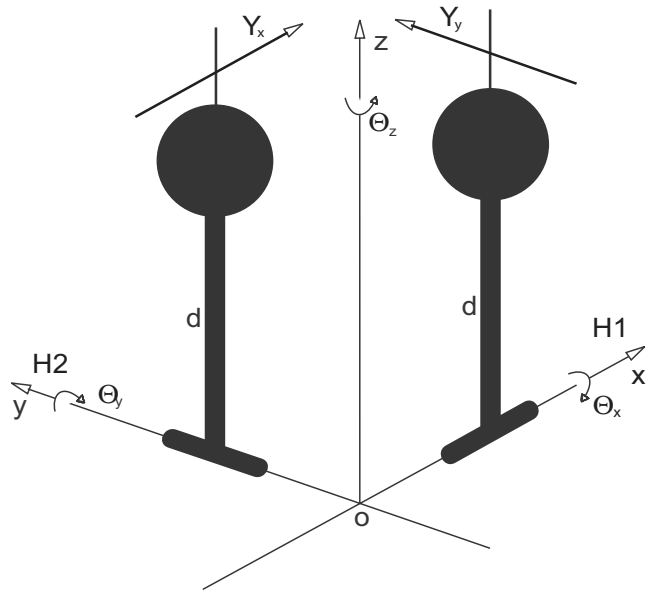

Figure 1. Schematic view of the two horizontal components of an inverted pendulum used in the Güralp Systems Limited CMG-40TOBS seismometer. d is the length of the pendulum arm. Yx and Yy are the two measurable displacements between frame and masses.

$$\ddot{Y}_x + 2\beta\omega_0\dot{Y}_x + \omega_0^2 Y_x = -\ddot{U}_x - d\ddot{\Theta}_y - g\Theta_y + g\Theta_z\Theta_x - \ddot{U}_z\Theta_y \quad \text{H1 component,} \tag{1}$$

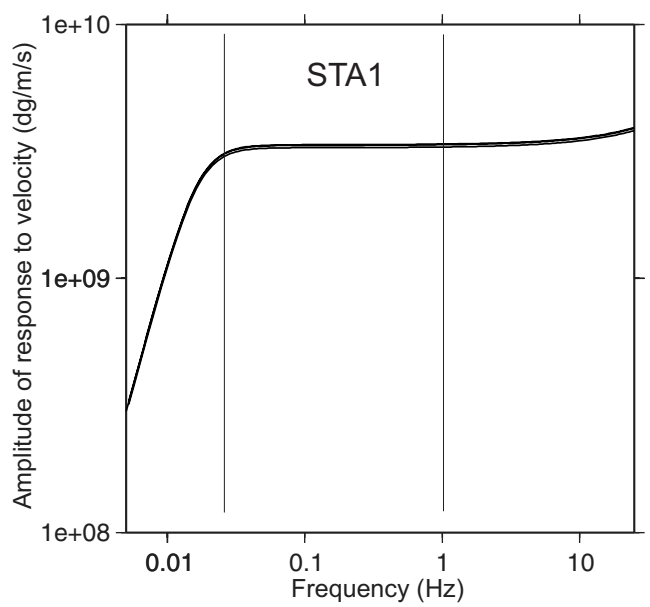

Figure 2. Velocity expressed bandwidth of the three components of the Güralp CMG-40TOBS seismometer taking into account the digitizer, the frequency response of which is flat. Our field of study will be limited to the frequency window between 0.02 and 1 Hz (50 to 1 sec).

$$\ddot{Y}_y + 2\beta\omega_0\dot{Y}_y + \omega_0^2 Y_y = -\ddot{U}_y + d\ddot{\Theta}_x + g\Theta_x + g\Theta_z\Theta_y + \ddot{U}_z\Theta_x \quad \text{H2 component,} \tag{2}$$

$$\ddot{Y}_z + 2\beta\omega_0\dot{Y}_z + \omega_0^2 Y_z = -g - \ddot{U}_z - d\ddot{\Theta}_x + 1/2g\Theta_x^2 + 1/2g\Theta_y^2 - \ddot{U}_y\Theta_x \quad \text{vertical component,} \tag{3}$$

where $Y_{i=x,y,z}$ are the measurable greatness of the inertial pendulum, β is the damping, and ω_0 is the natural pulsation defined by the electronic feedback. $U_{i=x,y,z}$ are the ground displacements along the indexed axis, g is the Earth's gravity (about 9.81 m/sec^2), d is the arm length in meters, and $\Theta_{i=x,y,z}$ is the rotation motion around the indexed axis.

For our purpose only, we use linear equations of the inverted pendulum. More complete equations of inverted pendulums are written by Graizer and Kalkan (2008) showing that pendulums can have nonlinear behavior at the tilt occurrence.

For the vertical component (equation 3), the second-order limited development of the cosine function (Streckeisen, 1983; Graizer, 2006) gives two terms: first, constant $-g$ and second, squared of the form $1/2\ g\Theta_x^2$ and $1/2\ g\Theta_y^2$.

The second-order cross-axis term $\ddot{U}_z\Theta_y$ for the H1 component and $\ddot{U}_z\Theta_x$ for the H2 component can be neglected; it is always smaller than the other term $g\Theta_y$and $g\Theta_x$ in small displacement conditions, and we neglect it in the following analysis.

The other terms $g\Theta_z\Theta_x$ and $g\Theta_z\Theta_y$ are also generally considered as secondary terms. They both show that the two horizontal component records contain the same torsion motion $g\Theta_z$ modulated by the tilt Θ_x for the H1 component and by the tilt Θ_y for the H2 component. The effect of these second-order terms ($g\Theta_z\Theta_x$ and $g\Theta_z\Theta_y$) is quite a bit smaller than the effect of the first-order terms ($g\Theta_y$ and $g\Theta_x$).

Nevertheless, these crossing terms can become first-order terms when seismometer installation tilt is large. Pillet and Virieux (2007) proposed that seismometer installation using bubble level protocol (or a gimbal tilt compensation in the OBS case) does not allow tilt to reduce lower than 10^{-3} radian, which is large compared to expected tilts produced by ground motion. Analyzing OBS data, we propose to separate these terms in two components: a large one associated with the installation tilt and a smaller one describing tilts under local ground deformation. The signal analysis will show that the first term can be predominant in the seismic band.

To analyze these equations and the importance of the different terms we suppose that, in general, conditions based on observation on land, rotation and translation motions in the seismic band (0.01–1 Hz) are of the same order of magnitude (10^{-8}).

Taking the Laplace transform of equations (1) and (2), we obtain an approximate solution to these equations if we separate out the response due to each effect (Rodgers, 1968). The transfer function for the acceleration terms becomes

$$F(s) = \frac{-s^2}{(s^2 + 2s\beta\omega_0 + \omega_0^2)}, \tag{4}$$

where acceleration terms are translation $U_{i=x,y,z}$ or angular motions $d\Theta_{i=x,y,z}$ as represented in Figure 3. This is the classical high-pass second-order filter that describes the seismometer band pass.

The transfer function for the rotational or tilting terms is

$$G(s) = \frac{-s^2 d + g}{(s^2 + 2s\beta\omega_0 + \omega_0^2)}. \tag{5}$$

According to this transfer function, the response to the tilt term is the sum of second-order filters (low and high-pass filter at the same frequency, Fig. 3). At low frequencies, the sensitivity to tilt is much larger than sensitivity to translation, and at high frequencies this term can be neglected. Data, in which we are interested, are only in the middle band where the signals can be of the same order.

The transfer function of the crossing term between torsion and tilt motions $g\Theta_z\Theta_x$ and $g\Theta_z\Theta_y$ for H1 and H2 components, respectively, is

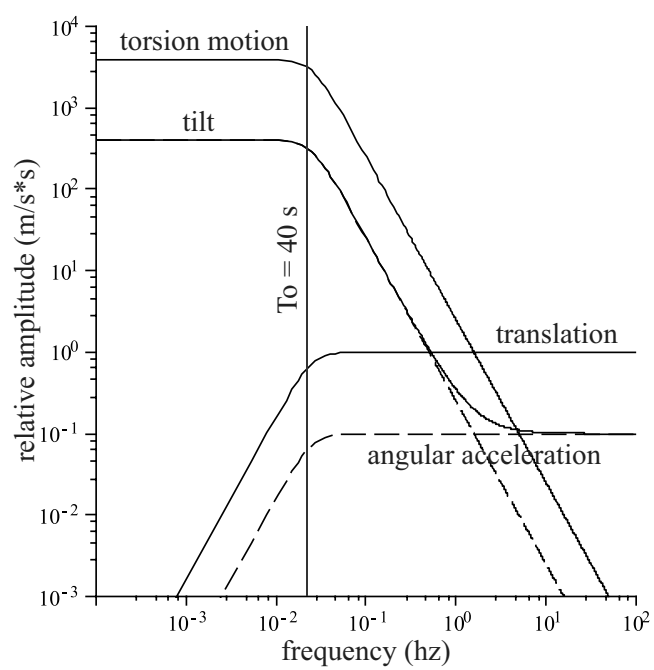

Figure 3. Log-log frequency response of the sensitive parameters: translation and rotations (tilt, angular acceleration, and torsion motion) recordings by a horizontal inverted pendulum of the CMG-40TOBS. If translation amplitude is 1 m/sec^2, rotational effect (tilt) is $g/2 = 397$ m (Rodgers, 1968) for $T_0 = 40$ sec. Torsion motion band-pass is plotted with an amplification factor of 10 to be more visible. This artificial amplification of the torsion motion band pass reflects the studied case where the torsion motion is prevailing on the tilt. Dashed lines representing tilt and angular acceleration are taken into account separately.

$$H(s) = \frac{g}{(s^2 + 2s\beta\omega_0 + \omega_0^2)}. \quad (6)$$

This transfer function (Fig. 3) is a low-pass second-order filter as computed by Rodgers (1968).

Seismic Noise Analysis

The three components recorded at OBS STA3 during the Rosmarin program (2006) show very strong background noise on the horizontal component (Fig. 4), especially for the long period. From 0.2 to 10 Hz, the background noise is halfway between the two curves NLNM and NHNM of Peterson (1993). Even though this noise is important, it remains within the usual limits of seismology, considering the fact that the instruments are just launched from the surface. On the other hand for periods longer than 5 sec, the OBS broadband background noise increases, whereas the terrestrial background noise is strongly reduced and exceeds the NHNM curve of Peterson (1993) by more than 60 dB. At the two others stations, similar curves are obtained.

Coherence between the Two Horizontal Components

We analyzed background noise sequences recorded by three Hippocampe OBS at STA1, STA2, and STA3 sites in 10 min long time windows. The time windows presented are selected among the 2 months of recording to be representative of the whole duration of the experiment avoiding specific high frequency noise often seen in seafloor data. The amplitude of raw data is almost five times larger at stations STA2 and STA3 compared to STA1, but the ratio between amplitudes on vertical and horizontal is the same. At frequencies lower than 0.2 Hz, the coherence between the two horizontal traces at station STA2 and STA3 is high and exceeds 95% (Figs. 5 and 6). At station STA1 (Fig. 7) the two horizontal traces present a globally lower coherence of about 70%, much less stable over the frequency band of the analysis. The amplitude difference between the two horizontal traces reaches a factor of 2 or more. The horizontal traces either have the same phase (STA2 and STA3) or are in phase opposition (STA1). In case of STA2 and STA3, the particle motion plots over the complete 10 min long time window show a clear, almost linear, polarization, which is very stable during the chosen time window. The particle motion plot for STA1 presents a global elliptical form much less stable in time as suggested by the lower and frequency dependent coherency.

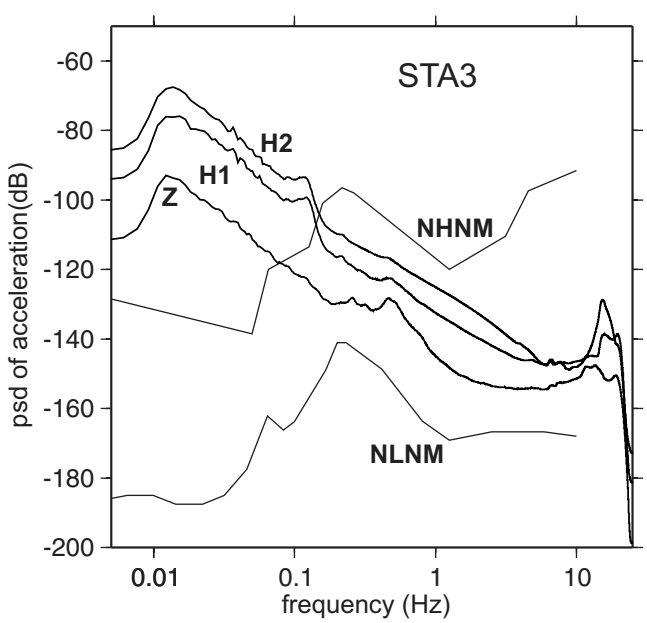

Figure 4. Three components (Z for the vertical component and H1, H2 for the two perpendicular components) background noise curves at site STA3. The spectral density of the noise is evaluated on a 12 hr time window taking into account the instrument transfer function of the CMG-40TOBS and the Hippocampe acquisition system. The amplitude is in decibels relative to $m^2/S3$, and the two NLNM, NHNM curves are from Peterson (1993). The long-period part, from 10 to 100 sec, presents an extremely strong background noise beyond the generally allowed maximum limit for terrestrial seismology.

Considering data at stations STA2 and STA3, where the noise is larger, the frequency band over which the high coherency between the two horizontal traces is observed (Figs. 5 and 6), is similar to the band over which $G(s)$, the transfer function related to the rotational motion (equation 6; Fig. 3), is larger than $F(s)$, the transfer function related to translation motion.

Coming back to the full horizontal pendulum (equations 1 and 2), the only common terms are the terms containing Θ_z rotation; therefore, we conclude that these terms are the predominant contribution to the horizontal signal that we observe at sites STA2 and STA3. Θ_z rotation is present through $g\Theta_z\Theta_x$ and $g\Theta_z\Theta_y$ terms, respectively, for H1 and H2 components, which means that Θ_z is modulated by Θ_x and Θ_y tilt motions.

Generally, these second-order crossing terms are considered to make a small contribution to the seismic signal compared to first-order tilt terms ($g\Theta_y$ and $g\Theta_x$). How can these observations be explained? How can a second-order term have larger amplitude than a first-order term? To answer this question, we are led to consider that the tilt breaks up into two components:

1. Installation tilt with having a large amplitude in OBS installations but staying stable at seismic frequencies;
2. Natural tilt induced by local deformations acting in the frequency band of the rotational motion (equations 4 and 5).

From this comment, rotational part of equation (1) becomes (same for equation 2) $g\Theta_z\Theta_{X\text{instal}} + g\Theta_z\Theta_{X\text{natural}} - g\Theta_{Y\text{instal}} - g\Theta_{Y\text{natural}}$ with:

1. A first, constant term that fixes the quadrant of the polarization. For example, STA1 and laboratory experiment

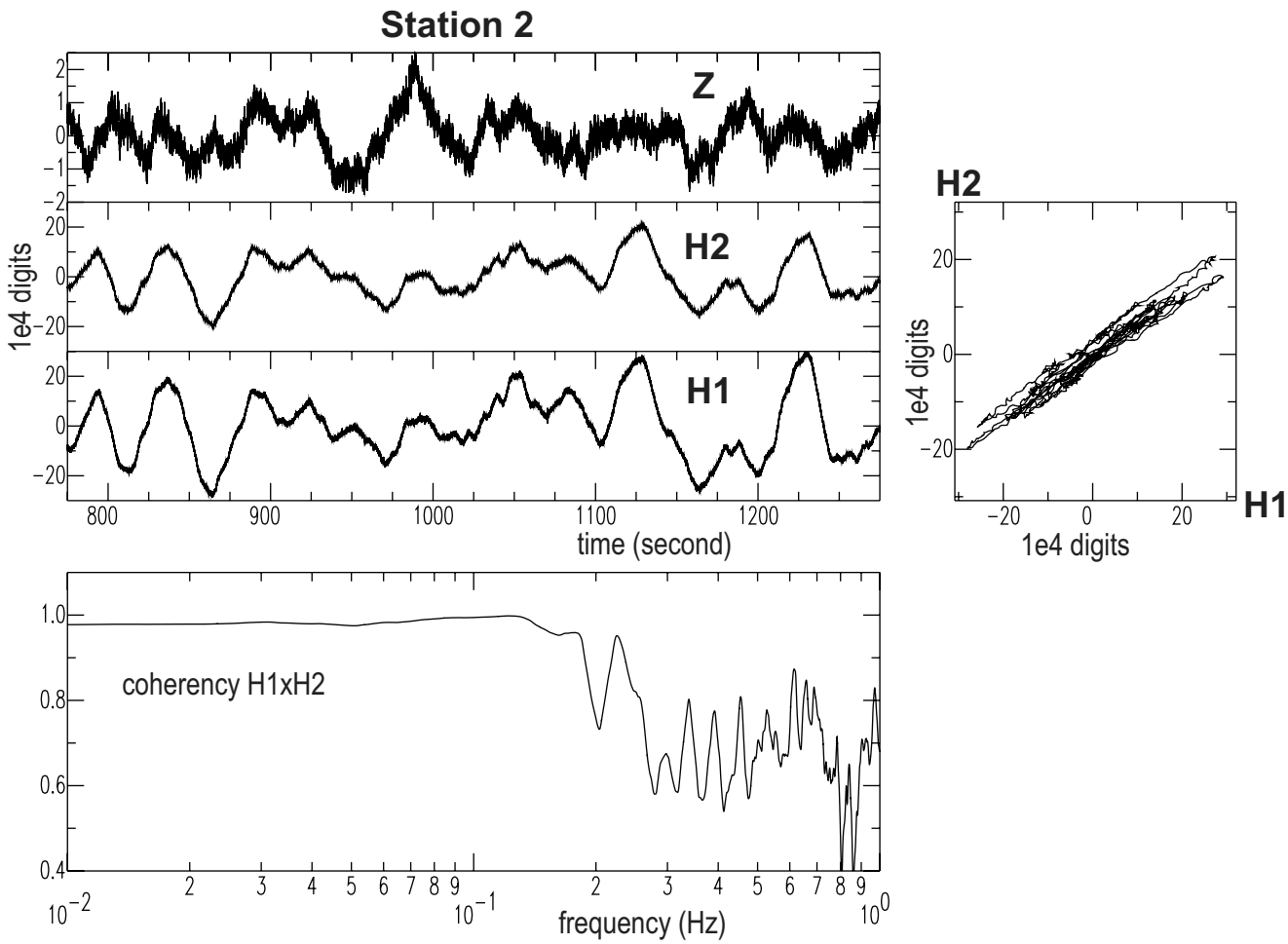

Figure 5. Analysis of 10 min time windows of background noise at station STA2. Raw data are presented in counts for the three components (the vertical component is 10 times smaller than the horizontal ones). On the right, the particle motion plot in the horizontal plane shows a clear horizontal polarization stable in that time window. The coherency between the two horizontal components is larger than 95% over a large frequency range (from 0.02 to 0.2 Hz).

(Figs. 7 and 8) show in the upper left polarization quadrant, whereas STA2 and STA3 (Figs. 5 and 6) show in the upper right polarization quadrant. The H1 and H2 components ratio is reversed because of the installation tilt polarity.

2. The second term is really a second-order term and negligible.
3. The third term is a constant producing the seismic signal offset, which cannot be distinguished by the numerical data logger or the nonzero pendulum rest position, and is neglected by seismologists.
4. Because the two horizontal components can be considered of similar magnitude, natural tilt (fourth term) must be less than the first term.

In our case, this second-order term is very important either because the installation tilts are strong, in spite of the use of improved gimbals, or because rotation Θ_z is particularly important compared to the other background noise components.

Installation tilt of the STA1 station is clearly better than the installation tilts of the STA2 and STA3 stations, and background noise of the STA1 station is largely built by the contribution of the first-order tilt term ($g\Theta_y$ and $g\Theta_x$).

If seismometer installation tilt remains stable over a given period, we will be able to measure their values and to correct the traces to make the amplitudes of the horizontal signals equal. So it would be possible to make the difference of the two balanced horizontal traces to remove the Θ_z term. The obtained seismic signal is not exploitable in terms of seismological signal except for a process of seismic detection of events, but seismic detection remains much better and more effective on the vertical component.

Laboratory Experiment

We performed a laboratory experiment, which consists of installing a CMG-40 seismometer (similar to the CMG-40TOBS) on a swivel table. Leveling of the sensor is per-

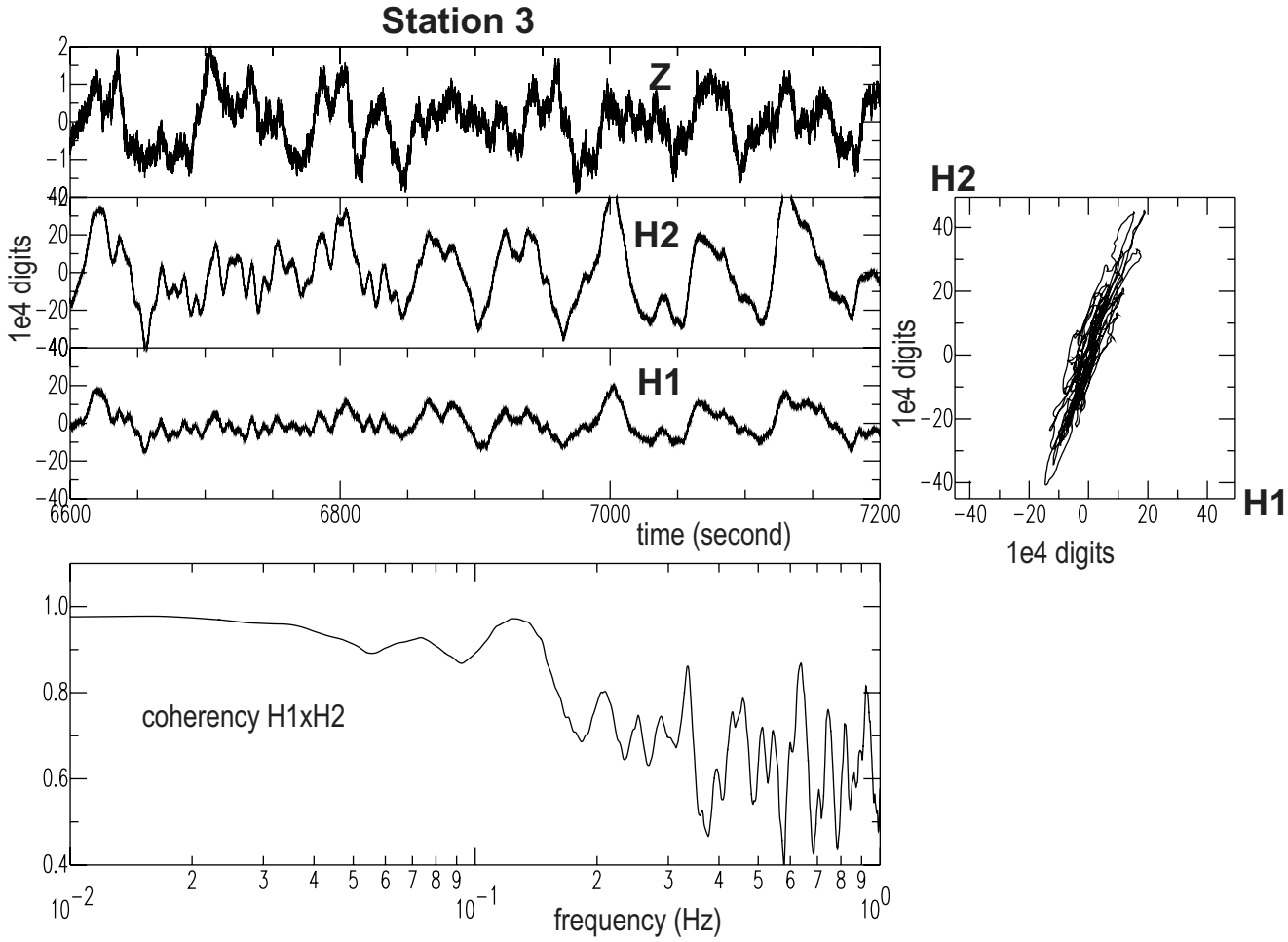

Figure 6. Same as Figure 5 for STA3. The relative amplitudes between horizontal components is different given a different angle on the particle motion plot. The coherency is somewhat smaller and the frequency band of the stable part shift toward longer periods.

formed by the bubble level included on the seismometer. The imposed rotation around the vertical axis is very strong and has an absolutely unspecified alternating rotating motion. The obtained raw signals are around 10 times larger in amplitude than the raw data recorded on OBS but are not clipped. The shape similarity between the two horizontal signals is clear in time domain. The coherency of the two raw horizontal signals is greater than 95% (Fig. 8), and the particle motion plot shows a very well defined and stable polarization. Reproducing such records after a different installation of the sensor, we show that the difference in amplitude of the horizontal components or the polarization direction is controlled by the installation static tilt. The similarity between these records and the OBS records supports our assumption that a large part of the noise observed on horizontal components of broadband OBS is due to the conjugate effect of a default of sensor leveling on the seafloor and of the noise of rotation around the vertical axis of the sensor (torsion motion). This tilt controls the torsional amplification factor. The corresponding frequency response is a second-order low-pass filter at the frequency of the pendulum. In spite of improved gimbals, we suspect that it remains a nonnegligible installation tilt of the sensor. The sensor housed in a 16 cm diameter spherical casing can bury itself when deployed to improve the ground coupling with the seafloor. But the small dimensions and spherical shape can also favor the coupling with seafloor water currents and can therefore increase the noise of the instrument.

Temporal Study of the Horizontal Seismic Noise

The STA3 OBS data analysis during the month of June 2006, performed on 2 hr time windows each day, shows large amplitude variations between the two horizontal traces. This amplitude variation is measured by processing the polarization azimuth of the particle motion in the horizontal plane (Fig. 9), and the horizontal components ratio varies from about 0.4 to 1.1. Study of 24 hr long time-windows records (23 June 2006) shows amplitude variation in the same scale with sometimes very high frequency jumps from a 1 hr time window to another. More fine study of two hours of signal (23 June beginning at 11 hr) with 600 sec processing time windows and with a 30 sec sliding time (to see the short-

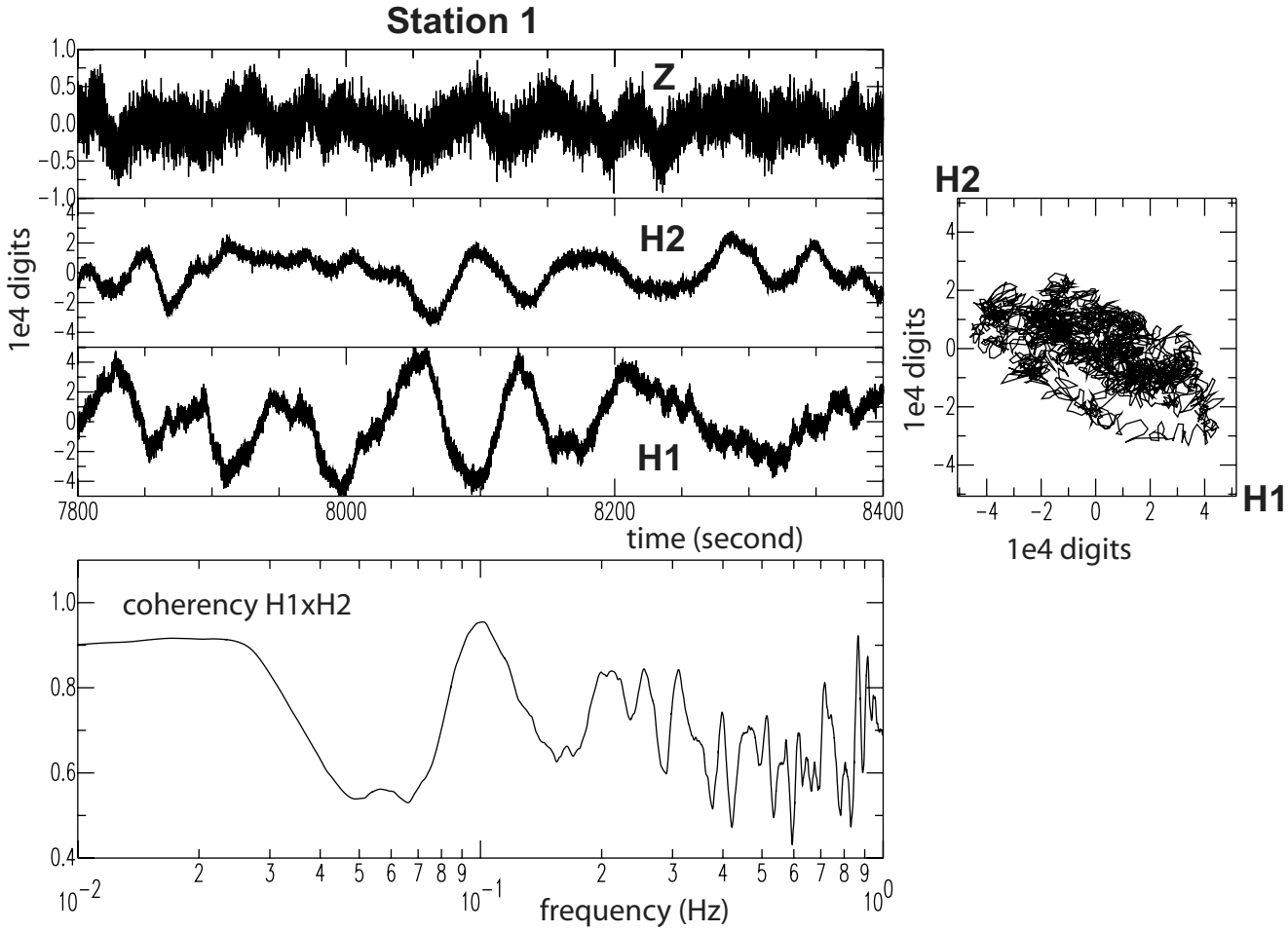

Figure 7. Same as Figures 5 and 6 for STA1. The amplitude of noise on the three components is almost five times smaller than on stations STA2 and STA3, but the relative amplitude between vertical and horizontal signals is conserved. The polarization of the plot particle motion is less pronounced than in the other examples; this feature is quantified by a coherency that is dependent of the frequency and not better than 75%.

period component of this phenomenon), shows fast jumps from a 1–3.5 amplitude ratio (Fig. 10). Temporal observations of Figure 10 show a wave shape always similar and a great amplitude ratio variation of the two horizontal traces.

To explain this result, we are obliged to consider that the H1 and H2 tilt terms, $g\Theta_y$ and $g\Theta_x$, respectively, have the same order amplitude as the crossed terms $g\Theta_z\Theta_{X\text{instal}}$ and $g\Theta_z\Theta_{Y\text{instal}}$.

Thus, the conjunction of tilt motion and torsion motion modulated by installation tilt led to results emphasized by Figure 10 where installation tilt fixes a medium value of the amplitude ratio (between the two horizontals traces) and where natural tilt disturbs the amplitude level of the two horizontal traces.

Installation tilt of the seismometer is great, constant in the time, and highlights the torsion motion. Natural tilt, also of great amplitude, disrupts the seismic traces through $g\Theta_y$ and $g\Theta_x$ terms. This great natural tilt is probably the result of poor ground coupling of the OBS station combined with seafloor currents.

Conclusion

The classical OBS recordings are known to be very sensitive to noise, and the new broadband OBS are even more so. On each recording of the 2006 Rosmarin operation stations (STA2 and STA3) the two horizontal traces presented rigorously identical signals, which are interpreted as a rotation around the vertical axis (torsion motion). This rotation is modulated by the seismometer installation tilt that modifies the amplitude of the two components. In the case of a rigorous installation, that is, with the removal of tilt, the two horizontal traces should not reveal this rotational signal around the vertical axis even if it is very strong.

Similarly, oil prospector's nodes OBS equipped with geophone do not see torsion motion because of the design of this sensor and of the more high frequency band pass. Our records are the conjunction between the inverted pendulum sensor that has the capability to record torsion motion at long period and between the presence of this torsion motion in the field. This torsion motion is perhaps an artifact induced by the weak coupling of the OBS on the seafloor. Maybe the

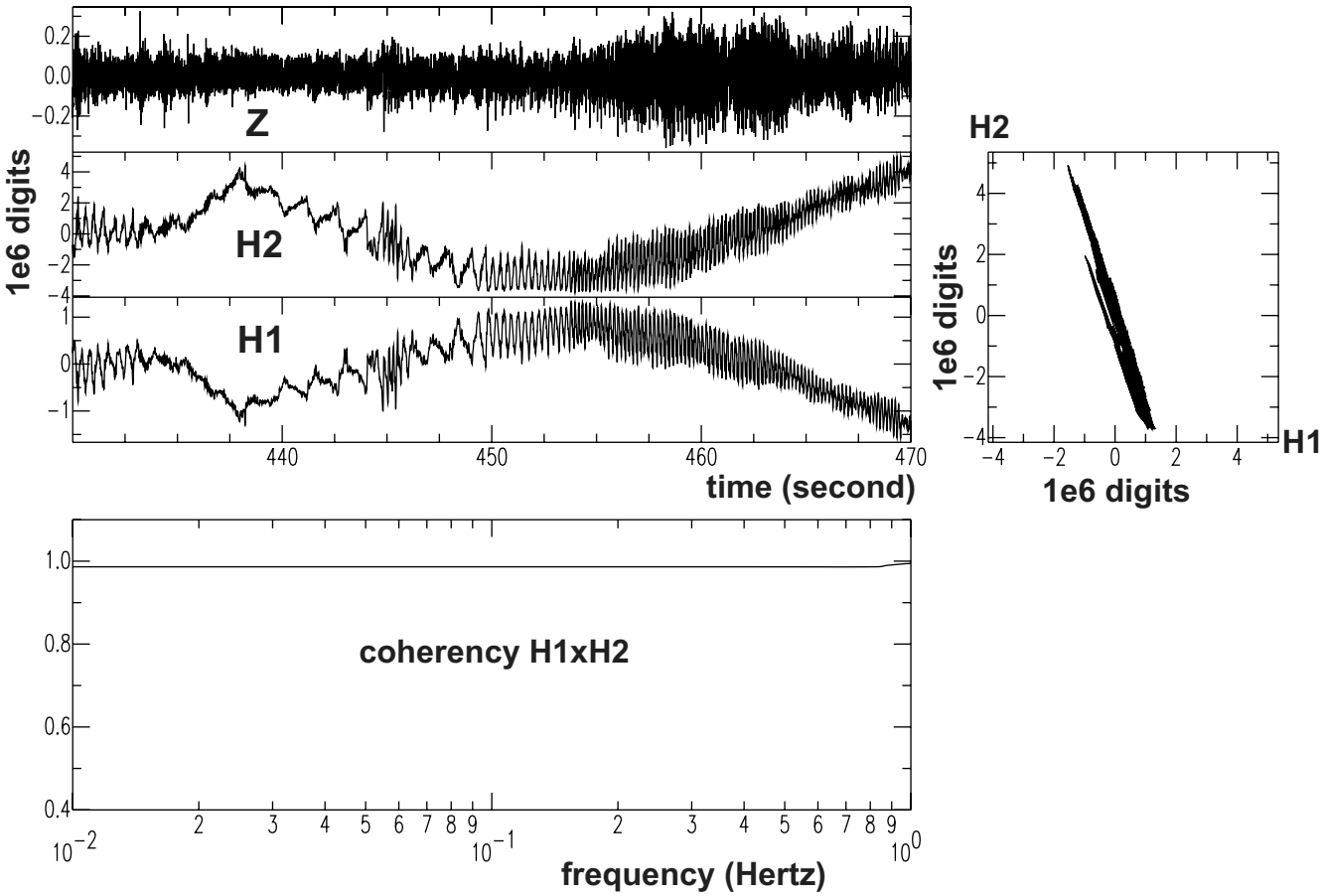

Figure 8. Analysis of 40 sec of the CMG-40 seismometer signal installed on a swivel table. The signal amplitude is close to saturation (10^6 counts). The raw installation according to the vertical axis and the resulting tilt explain the amplitude difference between the two traces. The resulting azimuth of the plot particle motion is an effect of the seismometer installation tilt. Coherency between the two horizontal traces is about 100%.

torsion effect can be due to local shear-wave-coupling heterogeneities as seen by oil prospectors (Paffenholz *et al.*, 2006a,b).

The technical manufacture of inertial translational sensors (seismometers) insensitive to rotations is impossible (Bradner and Reichle, 1973), but on the other hand, the feasibility of rotational sensors only sensitive to a single rotational degree of freedom is technically possible. The three rotational sensor addition, that is, a vertical axis and two orthogonal horizontal axes in parallel with the seismometers will make it possible to correct the seismic signals through removing the parasitic rotational signals. These signals of rotations will be used for the correction of all the terms of rotations which appear in equations (1) and (2). This will mean an even more significant reduction of the background noise than the method mentioned in this work. Crawford and Webb (2000) significantly corrected the vertical component using the horizontal traces that contain the tilt information at the first order (Rodgers, 1968).

The OBS recorded many parasitic movements: (1) because of the local conditions where the strong basic marine currents induce seismic noise more probably of rotation than of translation; (2) because of the installation protocol that implies a dubious coupling on the ground allowing possibilities of sensor motion, which is probably more important in rotation than in translation. We hope, and our study demonstrates, that under these extreme conditions, the principal source of background noise is due to the rotational motions rather than the translational one. A seismometer installation even more rigorous with regard to the vertical axis should reduce the term of coupling between the torsion and the tilt. The joint recordings of the three axes of rotation with rotational *ad hoc* sensors, sensitive only to one degree of freedom, will allow the corrections of the seismic traces and consequently bring about an important reduction of background noise.

From preceding information, it is difficult to propose a quantity to estimate the background noise reduction, but it seems clear that this noise reduction generated by applied rotational recordings and corrections will be very significant, and the OBS recordings could quickly join the quality of Earth stations and probably without changing the OBS deployment protocol.

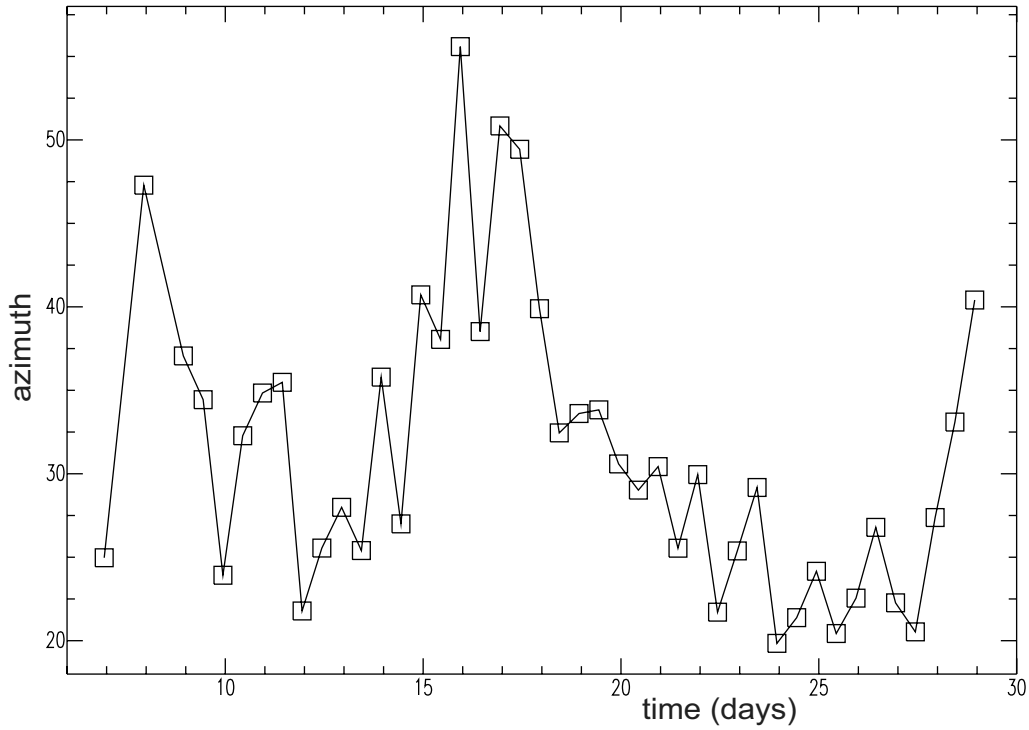

Figure 9. Temporal variation of the particle plot motion azimuth for the STA3 station during the month of June (from 7 to 29) with 2 hr time windows each day. Azimuth or amplitude ratio present a large variation.

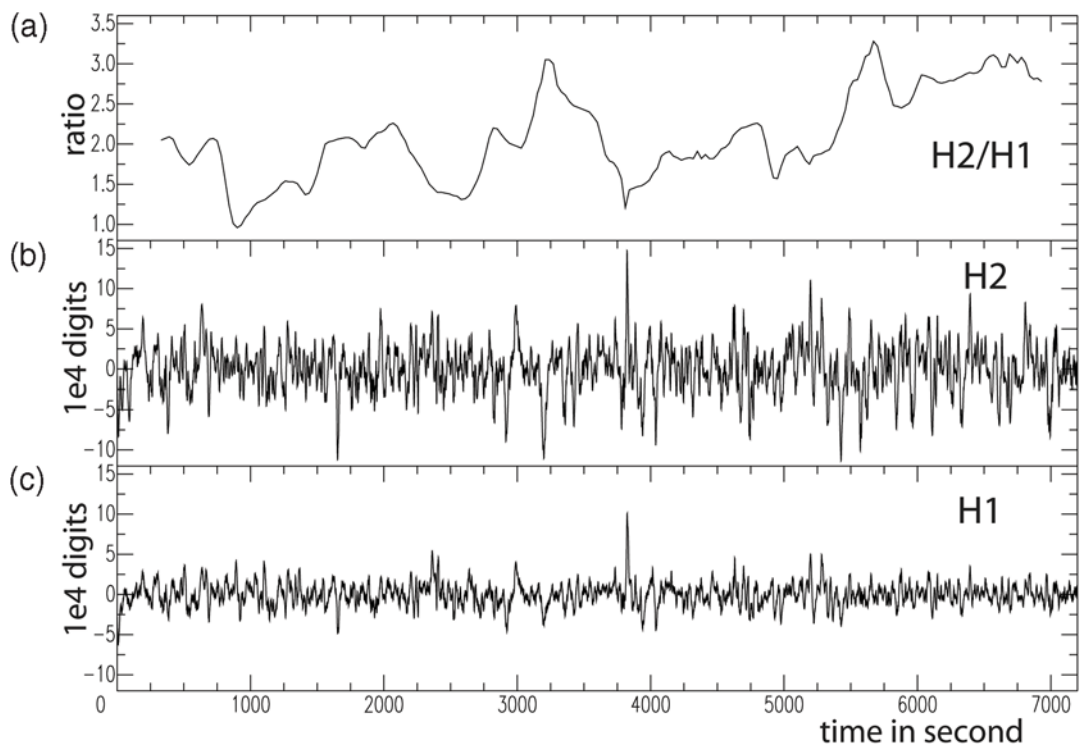

Figure 10. Temporal variation of the amplitude ratio of the two horizontal traces. (a) Amplitude ratio, (b) seismic horizontal traces for H2, and (c) for H1 are plotted on 2 hr long time windows (23 June 2006 beginning at 11 hr) expressed in seconds. Amplitude ratio is computed for time-windows analysis of 600 sec long, brought forward 30 sec each.

Data and Resources

Seismic data are analyzed using Seismic Analysis Code free software from Lawrence Livermore National Laboratory (P. Goldstein, A. Snoke, B. Savage, G. Helffrich, and R. Godbee).

References

Beaudouin, R., P. Lognonné, J.-P. Montagner, S. Cacho, J.-F. Karczewski, and M. Morand (1996). The effects of the atmospheric pressure changes on seismic signal or how to improve the quality of a station, *Bull. Seismol. Soc. Am.* **86,** 1760–1769.

Bradley, C. R., R. A. Stephen, L. M. Dorman, and J. A. Orcutt (1997). Very low frequency (0.2–10.0 Hz) seismoacoustic noise below the seafloor, *J. Geophys. Res.* **102,** no. 6, 11703–11718.

Bradner, H., and M. Reichle (1973). Some methods for determining acceleration and tilt by use of pendulums and accelerometers, *Bull. Seismol. Soc. Am.* **63,** no. 1, 1–7.

Byerly, P. (1952). Theory of the hinged seismometer with support in general motion, *Bull. Seismol. Soc. Am.* **42,** 251–261.

Charvis, P., and Y. Hello (2005). The new Hippocampe OBS and the French OBS pool, *Congressos UPC*, 1886–4864.

Crawford, W. C., and S. C. Webb (2000). Identifying and removing tilt noise from low-frequency (<0.1 Hz) seafloor vertical seismic data, *Bull. Seismol. Soc. Am.* **90,** 952–963.

Crawford, W. C., S. C. Webb, and J. A. Hildebrand (1991). Seafloor compliance observed by long period pressure and displacement measurements, *J. Geophys. Res.* **96,** no. 10, 16151–16160.

Dahm, T., F. Tilmann, and J. P. Morgan (2006). Seismic broadband ocean bottom data and noise observed with free-fall stations: Experiences from long-term deployments in the North Atlantic and Tyrrhenian Sea, *Bull. Seismol. Soc. Am.* **96,** no. 2, 647–664.

Galitzine, B. B. (1912). Lectures on seismometry, *Russ. Acad. Sci.*, St. Petersburg.

Galperin, E. I. (1985). Vertical Seismic Profiling and Its Exploration Potential, Series: Modern Approaches in Geophysics, Vol. **1,** Springer, 468 pp.

Graizer, V. M. (2005). Effect of tilt on strong motion data processing, *Soil Dyn. Earthq. Eng.* **25,** 197–204.

Graizer, V. M. (2006). Equation of pendulum motion including rotations and its implications to the strong-ground motion, *Earthquake Source asymmetry, Structural Media and Rotation Effects*, R. Teisseyre, M. Takeo, and E. Majewski (Editors), Springer, New York, 471–485.

Graizer, V., and E. Kalkan (2008). Response of pendulum to complex input ground motion, *Soil Dyn. Earthq. Eng.* **28,** 621–631.

LaCoste, L. (1934). A simplification in the conditions for the zero-length-spring seismograph, *Bull. Seismol. Soc. Amer.* **5,** 176–179.

Laske, G. (1998). Results from the Hawai SWELL experiment, in *EOS*American Geophysical Monograph **79,** no. 45, 662.

Longuet-Higgins, M. S. (1950). A theory of the origin of microseisms, *Phil. Tran. Roy. Soc.* **243,** 1–35.

Montagner, J.-P., J.-F Karczewski, B. Romanowicz, S. Bouaricha, P. Lognonné, G. Roult, E. Stutzmann, J.-L. Thirot, D. Fouassier, and J.-C. Koenig (1994). The French pilot experiment OFM/SISMOBS: First scientific results on noise level and event detection, *Phys. Earth Planet. Int.* **84,** 321–336.

Montagner, J.-P., B. Romanowicz, and J.-F. Karczewski (1994). A first step towards an oceanic geophysical observatory, in *EOS*, American Geophysical Monograph **75,** 150–154.

Paffenholz, J., P. Docherty, R. Shurtleff, and D. Hays (2006b). Shear wave noise on OBS Vz data-part II, elastic modelling of scatterers in the seabed, *EAGE, Expanded Abstracts*, **B047,** 631–635.

Paffenholz, J., R. Shurtleff, D. Hays, and P. Docherty (2006a). Shear wave noise on OBS Vz data-part I, evidence from field data, *EAGE, Expanded Abstracts*, **B046,** 625–630.

Peterson, J. (1993). Observation and modeling of seismic background noise, *U. S. Geol. Surv.Open-File Rept. 93-322*, Albuquerque, New Mexico, 1–95.

Pillet, R., and J. Virieux (2007). The effects of seismic rotations on inertial sensors, *Geophys. J. Int.* **171,** 1314–1323.

Rodgers, P. W. (1968). The response of the horizontal pendulum seismometer to Rayleigh and Love waves, tilt, and free oscillations of the Earth, *Bull. Seismol. Soc. Am.* **58,** no. 5, 1384–1406.

Romanowicz, B., D. Stakes, J.-P. Montagner, P. Tarits, R. Urhammer, M. Begnaud, E. Stutzmann, M. Pasyanos, J.-F. Karczewski, and S. Etchemendy (1998). MOISE: A pilot experiment towards long-term sea-floor geophysical observatories, *Earth Planets Space* **50,** 927–937.

Stephen, R. A., F. N. Spiess, J. A. Collins, J. A. Hildebrand, J. A. Orcutt, K. R. Peal, F. L. Vernon, and F. B. Wooding (2003). Ocean seismic network pilot experiment, *Geochem. Geophys. Geosyst.* **4,** no. 10, 1092, doi 10.1029/2002GC000485.

Streckeisen, G. (1983). Wide-band feedback seismometers, STS1-V/STS1-H, *Tech. Rep. Streckeisen Co.*, Pfungen, Switzerland.

Stutzmann, E., J.-P. Montagner, A. Sebai, W. C. Crawford, J.-L. Thirot, P. Tarits, D. Stakes, B. Romaniowicz, J.-F. Karczewski, D. Neuhauser, and S. Etchemendy (2001). MOISE: A prototype multiparameter ocean-bottom station, *Bull. Seismol. Soc. Am.* **91,** no. 4, 885–892.

Sutton, G. H., W. G. McDonnell, D. D. Prentiss, and S. N. Thanos (1965). Ocean bottom seismic observatories, in *Proc. Institute of Electrical and Electronics Engineers* **53,** 1909–1921.

Suyehiro, K., T. Kanazawa, N. Hara, and H. Kinoshita (1992). Broadband downhole digital seismometer experiment at site 794: A technical paper, in *Proc. Ocean Drilling Program, Scientific Results*, 127–128.

Trifunac, M. D., and M. I. Todorovska (2001). A note on the usable dynamic range of accelerograph recording translation, *Soil. Dyn. Earthq. Eng.* **21,** 275–286.

GéoAzur
Université de Nice Sophia-Antipolis, Institut de Recherche pour le Dévelopement, Centre National de la Recherche Scientifique,
Observatoire de la Côte d'Azur
250 rue Albert Einstein
Sophia-Antipolis
06560 Valbonne, France
pillet@geoazur.unice.fr
(R.P., A.D., J.V., N.B., B.Y.)

Geophysics Department
University of Chile
Blanco Encalada 2002
8370449 Santiago, Chile
(D.L.)

Manuscript received 2 June 2008